IOP Conference Series: Materials Science and Engineering

# A Numerical Investigation into the Impact of Icing on the Aerodynamic Performance of Aerofoils

To cite this article: Dinesh Bhatia and Al Yaqadan Shaaban al Wahaibi 2020 *IOP Conf. Ser.: Mater. Sci. Eng.* **831** 012007

# A Numerical Investigation into the Impact of Icing on the Aerodynamic Performance of Aerofoils

**Dinesh Bhatia**[1,a], **Al Yaqadan Shaaban al Wahaibi**[2]

[1]The University of Nottingham Ningbo China, School of Aerospace, 199 Taikang E. Road, Ningbo, China
[2]Military Technological College, Department of Aeronautical Engineering, 262 Al Matar Street, Muscat, Sultanate of Oman

[a] Corresponding author: Dinesh.Bhatia@nottingham.edu.cn

**Abstract.** Aircraft wings and wind turbine blades are often subjected to harsh and cold climatic conditions. Icing is often observed on wing and blade surfaces in these cold climatic conditions. Wind turbine blades, in particular, are severely impacted by ice accretion which greatly hampers their performance and energy generation efficiency. Ice-accretion patterns are observed to vary with changes in temperature. As the temperature changes, the thickness of the ice accretion, the shape and location of ice-accretion vary greatly. In this paper, three different ice accretion patterns and their impact on the aerofoil efficiency have been investigated using the SST $k-\omega$ model in ANSYS CFD. An analysis of the impact of ice-accretion through a comparison of lift and drag coefficients for all three ice accretion patterns indicate that the accretion of ice on an aerofoil can reduce lift generation by 75.3% and increase drag by 280% thereby severely impacting the performance of the aerofoil. The loss in aerodynamic performance is greatly dependent on the ridge height, the extent of ice accretion and the thickness of this ice. The loss in aerodynamic performance has no fixed correlation to the drop in temperature.

## 1. Introduction

Air-transportation and renewable energy generation has seen an exponential increase in their growth over the last two decades. With climate change being an ever-increasing reality, energy efficiency is the key to reduce global carbon emissions. Reduction in emissions from aircraft can be through improved aerodynamic performance and reduction in drag. In the case of wind turbines, a reduction in downtime can improve the efficiency of energy generation.

Aircraft are increasingly travelling to new destinations some of which are subject to extremely cold climatic conditions. Similarly, wind turbine installations are increasingly taking place in regions such as Greenland, Norway, Denmark, and Canada etc. which often face harsh winters. It is estimated that 24% of the installed wind power capacity is in cold regions where temperatures are often below 0℃ [1]. Icing has a very serious impact on the safety of aircraft and loss of power generation in the case of wind turbines. 240 cases of aviation accidents have been reported from 1990-2005 due to the presence of icing [2], [3]. Icing has also led to a 16% decline in the power generation capability of installed wind turbines [4]. Thus, it is imperative that the phenomenon of icing should be studied and remedial action taken to improve efficiency and safety of aircraft and wind turbines.

Icing on aerofoils has been studied extensively with a number ice-accretion experiments being conducted, details of which have been provided by Pouryussefi et al. [3]. One of the key outcomes from experimental testing of ice-accretion was the classification of the type of ice as well as the impact of non-dimensional ice height $(k/c)$ where k is the height/thickness of the ice accretion and c-chord length of the aerofoil. Ice can be classified into 5 main types based on the their shape: (1) roughness ice, (2) horn ice, (3) streamwise ice, (4) spanwise ridge ice, and (5) runback ice [5]. Wind tunnel tests indicate that presence of icing can reduce the lift coefficient within a range of 50- 60% as compared to a clean aerofoil although the data for the increase in drag coefficient is not readily available [3], [5]. While the impact of ice-accretion has been quantified experimentally, the use of simulations to quantify this effect has been few and far between. Simulations have usually been conducted using LES and DNS and user defined CFD models which make them time-consuming.

The purpose of this paper is to quantify the effects of three classical ice-shapes namely Ice Shape 290, 296 and 312 accurately, reliably and quickly on the lift and drag of a NACA23012 aerofoil numerically using a commercial CFD software (ANSYS). Details of these ice shapes are readily available in literature [5]. The impact of the ice height and location will also be studied.

This paper aims to demonstrate the viability of using a commercial CFD software along with a readily available CFD model (the SST $k-\omega$ model) to ensure rapid and accurate results for quantifying the impact of ice accretion on aerofoils. The paper will also provide the basic reference for any future study aimed at quantifying the impact different ice-accretion scenarios on the aerofoil performance.

## 2. Methodology

### *2.1. Mesh Generation*

2D simulations were conducted and results were computed using the $k-\omega\ SST$ Turbulence model in ANSYS FLUENT. The meshing was carried out using the default workbench meshing software in ANSYS. NACA 23012 was chosen as the default aerofoil for the simulations and ice accretion profiles were digitised based on profiles obtained from existing wind tunnel ice accretion tests by Broeren et al. [5] as shown in Figure 1.

The aerofoil is assumed to have a chord length of 1.0 metre with the origin at the leading edge (0,0,0) and the trailing edge to be at (1,0,0). The meshing criteria was selected based on the mesh parameters set by Parashar [6].

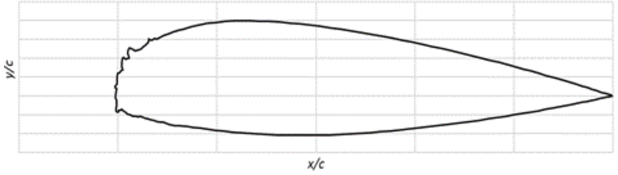

**Figure 1.** Digitised Ice Shape 290 from existing experimental data

The computational domain was set to be 20c (c-chord length of the aerofoil) upstream and downstream. A no-slip wall boundary condition was used on all solid boundaries whereas a farfield condition was set for the upper and lower boundaries. The boundary on the left was set as a velocity inlet whereas the one on the right was set to be a pressure outlet. A hybrid grid mesh was used with a $y^{+}=1.0$ near the aerofoil walls and a wall expansion ratio of 1.07. A mesh-independence check was conducted, and it was found that a mesh with 59,000 elements produced a truly mesh-independence solution.

Figure 2 shows an example of a mesh around a digitised iced aerofoil with a structured mesh around the aerofoil to resolve the boundary layer and an unstructured mesh further away from aerofoil.

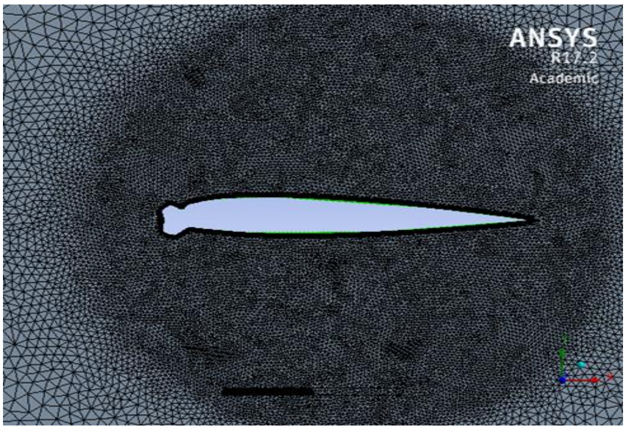

**Figure 2.** Hybrid mesh around a digitised iced aerofoil

### *2.2. Validation*

Validation of the simulations were conducted against experimental tests done by Pouryoussefi et al. at a Reynolds number of $0.6 \times 10^6$ keeping all other parameters constant [3]. Plots of the lift coefficient $C_l$ vs. the angle of attack $\alpha$ and the drag coefficient $C_d$ vs. the angle of attack $\alpha$ were plotted for the NACA23012 aerofoil to obtain good correlation between the simulation method and experimental data. The plots are shown in Figure 3 below.

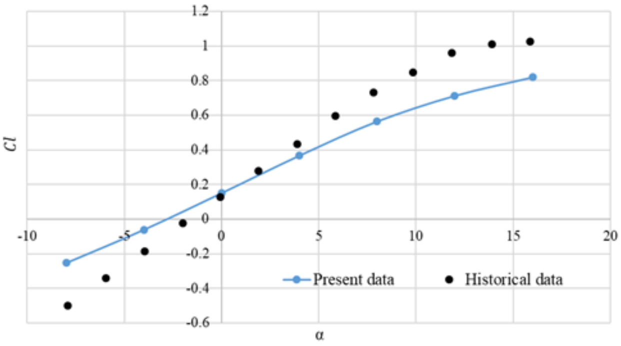

(a) $C_l$ vs. $\alpha$ for simulated data vs experimental data

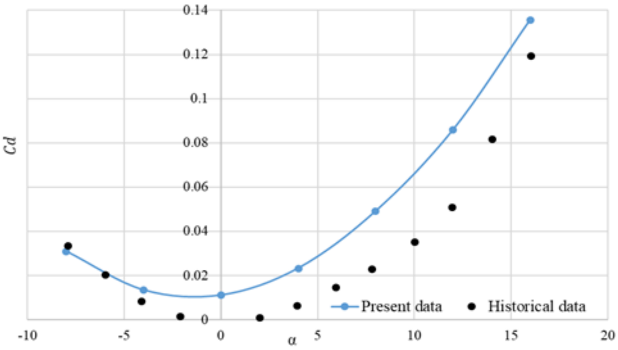

(b) $C_d$ vs. $\alpha$ for simulated data vs experimental data

**Figure 3.** Lift and Drag Coefficients for simulated data vs. historical experimental data for NACA23012

Data presented in Figure 3 shows good correlation and a very similar trend between the experimental tests conducted by Pouryouseffi et al. and the simulations conducted by the authors. Variations between the experimental and simulated data could be put down to a few unknown factors such as the use of 2D simulations as well as temperature, density and the turbulence level at which the experiments were conducted. Temperature, density and turbulence were kept at default values during the simulations by the authors.

## 3. Results and Discussion

Three classical icing scenarios were considered in order to analyse their aerodynamic performance vs. the clean aerofoil. Ice Shape 290, 296 and 312 were considered based on the type of ice, location of the ice ridge on the aerofoil along with the height of the ice ridge.

Table **1** provides specific details about these ice shapes whereas Figure 4 shows the specific shapes from existing experimental data [7].

**Table 1.** Test conditions and specifications for different ice-shapes

| Ice-Shape | T (K) | Ridge Height (k/c) | Location (x/c) |
|---|---|---|---|
| 290 | 263 | 0.0138 | 0.020 |
| 296 | 268 | 0.0122 | 0.035 |
| 312 | 258 | 0.0131 | 0.060 |

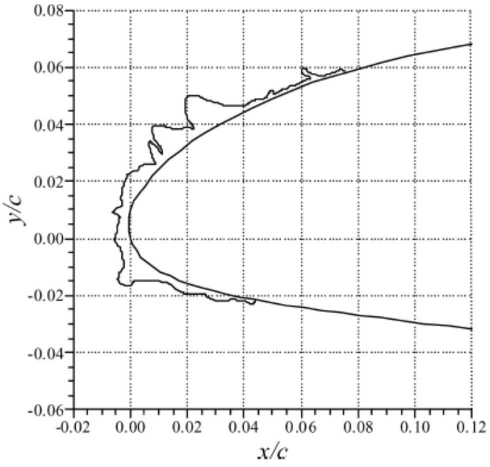

(a) Ice-Shape 290

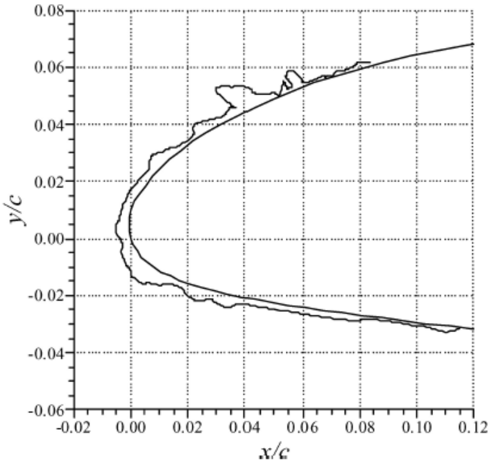

(b) Ice-Shape 296

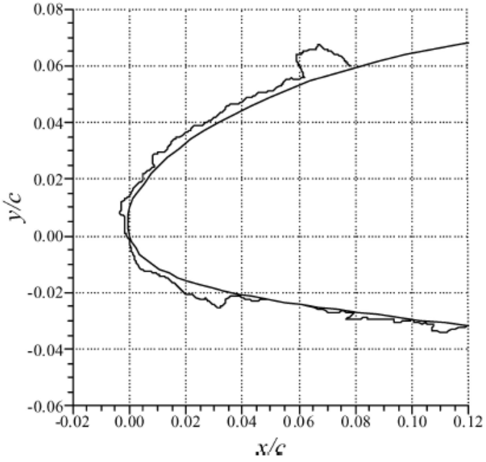

(c) Ice-Shape 312

**Figure 4.** Ice Shapes 290, 296 and 312 depicting different ice accretion patterns [7]

All three ice-shapes represent vastly different locations for ice-accretion based on the temperature. The temperature also impacts the type of ice that accumulates on the aerofoil. Ice-shape 290 represents a mixed glaze-rime shape which leads to substantial ice-accumulation closer to leading edge. Ice-shape 296 and 312 are glaze shaped ice with different locations and height for the ridge shaped ice accretions. The presence of these different ridge shaped ice-accretions greatly impacts the aerodynamic performance of the aerofoils.

A comparison of the lift coefficient $C_l$ vs. the angle of attack $\alpha$ (shown in Figure 5 ) indicates that the ice-shapes 296 and 312 have very similar performance, but show a 60% reduction in lift as compared to the clean aerofoil. On the other hand, ice-shape 290 has the greatest lift reduction of about 75% as compared to the clean aerofoil. A very crucial factor that affects the performance is the height of ice-shape, with an increase in the height greatly reducing the lift coefficient $(C_l)$. Ice-shape 290 had the largest ridge height of $k/c = 0.0138$ which resulted in significant drop in the lift coefficient $(C_l)$. The lift coefficient $(C_l)$ is marginally higher for ice-shape 312 which can be attributed to the fact the ridge of the ice is located the furthest away from the leading edge at $\left({}^{x}/_{c}\right) = 0.060$ .

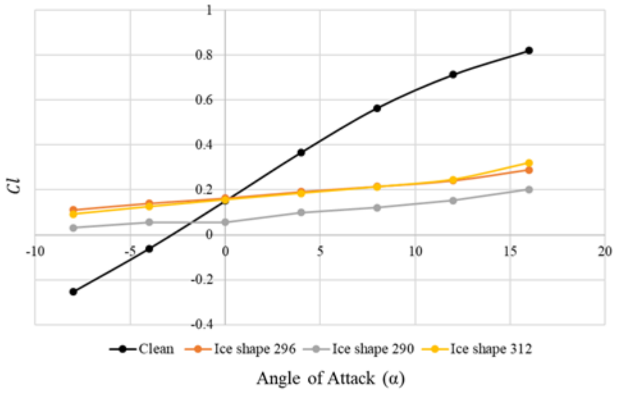

**Figure 5.** Lift coefficient comparison for three different ice-shapes vs. the clean aerofoil

A comparison of the drag coefficient $(C_d)$ vs. the angle of attack $\alpha$ (shown in Figure 6 ) indicates that ice-shape 312 has the highest drag as compared to the clean aerofoil. Ice-shape 290 has the highest ridge height but the lowest extend of ice accretion around the upper and lower surfaces of the aerofoil whereas ice shape 296 has the lowest ridge height but the extent of ice accretion around the aerofoil extends upto $\left({}^{x}/_{c}\right) = 0.11$ on the lower surface albeit with an overall lower thickness as compared to ice-shape 290.

This possibly results in the lowest drag amongst the three ice-shapes. In the case of ice-shape 312, the ridge is located the furthest along the aerofoil at $(^{x}/_{c}) = 0.060$ , the extent of the ice accretion is the furthest until $(^{x}/_{c}) = 0.12$ on the lower surface. A combination of the second highest ridge height and the largetst extent of ice-accretion along the aerofoil in the streamwise direction might have contributed to a higher drag for ice-shape 312 as compared to the clean aerofoil. In the case ice-shape 312, the drag is 280% higher than in the case of the clean aerofoil thereby indicating a significant loss in aerodynamic performance.

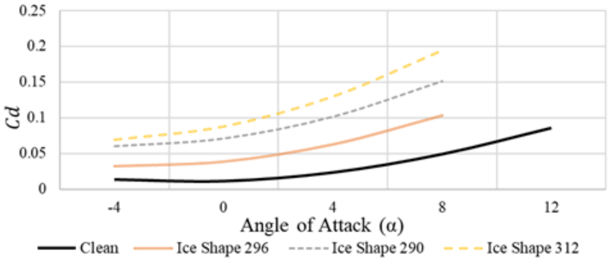

**Figure 6.** Drag coefficient comparison for three different ice-shapes vs. the clean aerofoil

Table 2 Summarises the relative performance of the aerofoil for the three different ice shapes vs the clean aerofoil.

Finally, a comparison between the boundary layer thickness of Ice shape 290 vs. the clean aerofoil was conducted as shown in Figure 7 and highlights the impact that ice accretion has on the overall flow structure. Ice shape 290 was used as it had the highest ridge height but the lowest overall ice extent over the aerofoil. For Ice Shape 290, the maximum ridge height is at $x/c = 0.08$. At this point, a comparison of the boundary layer thickness between Ice Shape 290 and the clean aerofoil indicates that the boundary layer for Ice Shape 290 is about 60% thicker which indicates a less streamlined fluid flow. The boundary layer thickness beyond the ice accretion area at $x/c = 0.2$ tends to show similar thickness. At this point, the Ice Shape 290 has an 8.6% thicker boundary layer. However, along the entire length of the aerofoil, Ice Shape 290 tends to depict a much thicker boundary layer as compared to the clean aerofoil which is a clear indicator of a less streamlined flow.

**Table 2**. Relative performance comparison between the iced-aerofoil and the clean aerofoil

| Ice-Shape | Lift Decrease (%) | Drag Increase (%) |
|---|---|---|
| 290 | 75.3 | 200 |
| 296 | 64.8 | 120 |
| 312 | 60.9 | 280 |

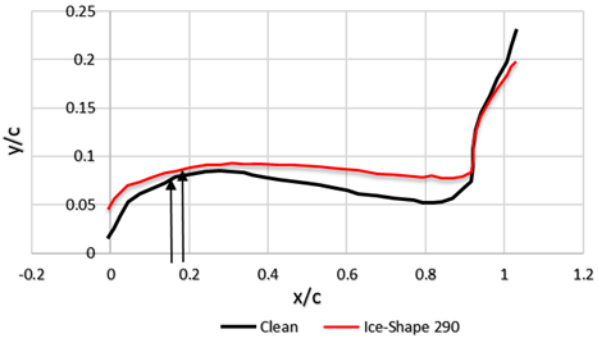

**Figure 7.** Boundary layer thickness comparison between clean aerofoil and Ice Shape 290

## 4. Conclusions

The impact of ice-accretion on aerofoils was studied numerically. The aerodynamic performance of three different classical ice accretion profiles namely ice-shapes 290, 296 and 312 were simulated using the SST $k-\omega$ model within a commercial CFD software and their results were compared to a clean NACA23012 aerofoil. Results indicate that the aerodynamic performance of an iced aerofoil is greatly impacted by the ridge height (k/c), the extent of ice accretion on the aerofoil surface as well as the thickness of this ice accretion. A larger concentration of ice around the leading edge (ice-shape 290) leads to a significant drop in the lift but doesn't necessarily lead to the largest increase in drag. However, the impact of the accumulated ice is observed along the entire length of the aerofoil and manifests itself in the form of a thicker boundary layer. A combination of the extended accumulation of ice (as seen in ice-shape 312) along with the presence of a ridge at the end of the ice accretion region leads to a significant increase in drag.

There is no fixed correlation between a drop in the temperature and the loss of aerodynamic performance. The substantial increase in drag and the drop in lift has great repercussions for the smooth operations of aircraft as well as wind turbines. Effective solutions are essential for anti-icing of the aerofoil or to de-ice the aerofoil surface once the ice has accumulated without significant consumption of energy as that will greatly impact the overall efficiency of the aircraft or wind turbine

The use of the SST $k-\omega$ model and a commercial CFD software have shown to provide rapid, reliable and repeatable results that should enable quantification of performance loss in a wide range of ice accretion scenarios.

## 5. References

[1] A. Hudecz, "Icing Problems of Wind Turbine Blades in Cold Climates," Technical University of Denmark, 2014.

[2] J. Mason, W. Strapp, and P. Chow, "The Ice Particle Threat to Engines in Flight," in *44th AIAA Aerospace Sciences Meeting and Exhibit*, 2006.

[3] S. G. Pouryoussefi, M. Mirzaei, M.-M. Nazemi, M. Fouladi, and A. Doostmahmoudi, "Experimental study of ice accretion effects on aerodynamic performance of an NACA 23012 airfoil," *Chinese J. Aeronaut.*, vol. 29, no. 3, pp. 585–595, Jun. 2016.

[4] "Wind Energy in Cold Climates | Natural Resources Canada," *Natural Resources Canada*, 2017. [Online]. Available: https://www.nrcan.gc.ca/energy/energy-sources-distribution/renewables/wind-energy/wind-energy-cold-climates/7321. [Accessed: 19-Jul-2019].

[5] A. P. Broeren, E. A. Whalen, G. T. Busch, and M. B. Bragg, "Aerodynamic Simulation of Runback Ice Accretion," *J. Aircr.*, vol. 47, no. 3, pp. 924–939, May 2010.

[6] H. Parashar, "Calculation of Aerodynamic Characteristics of NACA 2415, 23012, 23015 Airfoils Using Computational Fluid Dynamics (CFD)," *Int. J. Sci. Eng. Technol. Res.*, vol. 4, no. 3, pp. 610–614, 2015.

[7] A. P. Broeren, M. B. Bragg, and H. E. Addy, "Effect of Intercycle Ice Accretions on Airfoil Performance," *J. Aircr.*, vol. 41, no. 1, 2004.